

Glycogen synthase kinase 3 promotes the proliferation of porcine epidemic diarrhoea virus by phosphorylating the nucleocapsid protein

Xiangchao Jia^a, Jing Chen^a, Chenxi Li^a, Jian Li^a, Min Su^a, Kang Yang^a, Yang Zhang^a, and Zili Li ^{a,b}

^aState Key Laboratory of Agricultural Microbiology, College of Veterinary Medicine, Huazhong Agricultural University, Wuhan, Hubei, China;

^bKey Laboratory of Preventive Veterinary Medicine in Hubei Province, Huazhong Agricultural University, Wuhan, Hubei, China

ABSTRACT

Porcine epidemic diarrhoea virus (PEDV) is a highly pathogenic porcine enteric coronavirus that causes severe watery diarrhoea and mortality in piglets. The nucleocapsid protein (N) is the most abundant viral protein and is highly phosphorylated, with the phosphorylation level directly affecting infection and proliferation. Here, we characterized the phosphorylation level of the N protein and found that its SR (Ser and Arg) motif was highly phosphorylated. The phosphorylation level significantly decreased after mutation of threonine (Thr) to serine (Ser). Through screening, it was determined that GSK3 α/β plays a major role in phosphorylating the SR motif. Using GSK3 α/β inhibitors or directly knocking out the GSK3 α/β gene significantly inhibit PEDV proliferation. Finally, we used yeast recombination technology to develop a reverse genetics system for assessing PEDV and confirmed that no differences existed between the wild-type strain and the rescued virus. Using this platform, we generated a PEDV N protein SR motif mutant strain. We found that, compared to the wild-type strain, the proliferation of the mutant strain was significantly weakened, confirming that the phosphorylation of the SR motif is crucial for PEDV proliferation. In summary, we verified the phosphorylation sites of the PEDV N protein and the associated protein kinases, providing new insights into the development of relevant therapeutic strategies.

ARTICLE HISTORY

Received 3 January 2025

Revised 10 April 2025

Accepted 27 April 2025

KEYWORDS

Coronavirus; porcine epidemic diarrhoea virus; phosphorylation; glycogen synthase kinase 3; infectious clone

Introduction

The coronavirus nucleocapsid (N) protein is the most abundant and strongly expressed protein during the viral life cycle [1,2]. The N protein interacts with the viral genomic RNA to form a ribonucleoprotein complex that stabilizes the viral genome. Additionally, the N protein plays an important role in the synthesis of viral RNA and proteins, as well as in virus packaging and budding processes [3,4]. The N protein of the porcine epidemic diarrhoea virus (PEDV) is composed of 435 amino acids, with an N-terminal structure involved in RNA binding [5,6] and a C-terminal that promotes protein oligomerization [7,8]. The central region contains a motif rich in serine (Ser) and arginine (Arg) (SR), which is highly conserved in coronaviruses [9]. Notably, the N protein of coronaviruses is highly phosphorylated [10], with phosphorylation occurring mainly at the Ser and Thr residues [11–14].


The phosphorylation level of the N protein may affect its activity and subcellular localization [10,15]. The proteins are modified by hijacking the host protein kinase system to promote viral replication and

assembly. Chen and colleagues found that phosphorylated IBV nucleocapsid proteins exhibit a higher viral RNA-binding capability [12]. Phosphorylation of the MHV N protein can recruit the DDX1 helicase and enhance the transcription of viral RNA [16]. Phosphorylation of the SARS and SARS-CoV-2 N proteins is related to glycogen synthase kinase 3 (GSK3), and inhibiting the activity of GSK3 can impair SARS-CoV and SARS-CoV-2 infections in target cells [9,17,18].

Reverse genetic systems are important tools in viral research and vaccine development. Currently, there are four main types of reverse genetics systems for coronaviruses: targeted RNA recombination techniques [19], viral cDNA linked to bacterial artificial chromosomes (BAC) [20–22], in vitro ligation of cDNA fragments to construct full-length infectious clones [20], and infection clones based on yeast recombination technology [23]. Among these, yeast recombination technology can significantly reduce the instability of cDNA clones [24] and is fast and convenient to operate [25,26].

In this study, a Phos-tag gel was used to analyse the phosphorylation level of the PEDV N protein,

CONTACT Zili Li  lizili@mail.hzau.edu.cn

 Supplemental data for this article can be accessed online at <https://doi.org/10.1080/21505594.2025.2506504>

© 2025 The Author(s). Published by Informa UK Limited, trading as Taylor & Francis Group.

This is an Open Access article distributed under the terms of the Creative Commons Attribution-NonCommercial License (<http://creativecommons.org/licenses/by-nc/4.0/>), which permits unrestricted non-commercial use, distribution, and reproduction in any medium, provided the original work is properly cited. The terms on which this article has been published allow the posting of the Accepted Manuscript in a repository by the author(s) or with their consent.

demonstrating that the SR motif of the N protein was highly phosphorylated. Host GSK3 plays an important role in phosphorylating the SR region. GSK3 is a ubiquitously expressed Thr/Ser kinase with two isoforms, GSK3 α and GSK3 β . Using GSK3 α/β inhibitors or knocking out the GSK3 α/β genes impairs PEDV proliferation in Vero and IPI-2I cells. Finally, we used yeast recombination technology to construct a PEDV N protein SR motif mutant strain, and its proliferation was significantly weakened compared to that of the wild-type strain.

Materials and methods

Cells and virus

IPI-2I cells were provided by Prof. L. Zhang at Huazhong Agricultural University. HEK-293T, BHK-21, and Vero cells were stored in our laboratory [27–29]. HEK-293T, Vero, BHK-21, and IPI-2I cells were cultured in DMEM (HyClone, Logan, UT, USA) containing 10% FBS (Life Technologies, Grand Island, NY, USA) and 1% penicillin-streptomycin [29]. All cells were cultured in an incubator at 37°C, 5% CO₂. PEDV strain JS-A (GenBank mh748550.1, <https://www.ncbi.nlm.nih.gov/nucleotide/mh748550.1>) was propagated in IPI-2I cells [29].

Antibodies and reagents

Mouse or rabbit monoclonal antibodies (mAb) against FLAG (Catalog No. AE092) and HA (Catalog No. AE008), mouse anti-glyceraldehyde phosphate dehydrogenase (GAPDH) mAb (Catalog No. AC002), horseradish peroxidase (HRP)-labelled goat anti-mouse (Catalog No. AS003) or rabbit (Catalog No. AS014) IgG (H+L), ABflo® 594-conjugated goat anti-rabbit (Catalog No. AS039), ABflo® 488-conjugated goat anti-mouse IgG (H+L) (Catalog No. AS037), GSK3 α rabbit mAb (Catalog No. A19060), and GSK3 β rabbit mAb (Catalog No. A11731) were purchased from ABclonal (Wuhan, China). The mouse mAb against the PEDV N protein was maintained by our laboratory. Polyclonal antibody against the PEDV N protein was preserved in our laboratory. GSK3 α/β inhibitors CHIR-99021 HCl (Catalog No. T2310L), SB 216763 (Catalog No. T3077), and TWS119 (Catalog No. T2166) were purchased from TargetMol (Shanghai, China). LiCl (Catalog No. ST498), λ PPase (Catalog No. P2316S), and cell lysis buffer for Western blotting and Co-IP (RAPI) were acquired from Beyotime (Shanghai, China). The Lipofectamine 3000 transfection reagent (Catalog No. L3000008) was purchased from Invitrogen (Carlsbad, CA, USA). Cell Counting Kit-8 (CCK-8; Catalog No. BS350A) was

obtained from Biosharp (Hefei, China). 4',6-Diamidino-2-phenylindole dihydrochloride (DAPI; Catalog No. C0065) was purchased from Solar Bio (Beijing, China). Protein Marker (Catalog No. MP102) and Phos-Assay Acrylamide (Catalog No. PA101) were acquired from Vazyme (Nanjing, China).

Construction of PEDV infectious clone plasmids and rescue of recombinant viruses

The genome of the PEDV JS-A strain was divided into seven parts, which were amplified using the primers listed in Table 1, with an overlapping region of 100–200bp between each fragment. The CMV promoter and HDV-BGH transcription termination sequences were added to the yeast vector pYES1L-URA (Catalog No. 84301, Addgene), and the resulting vector was named pYES1L-CMV-BGH. We co-transformed the linearized pYES1L-CMV-BGH vector with the seven amplified PEDV gene fragments into Mav203 competent cells. Positive colonies were identified using the primers listed in Table 2, and plasmids were extracted for sequencing. Plasmids containing the correct sequences were electroporated into DH10B competent cells for large-scale amplification. BHK-21 cells were seeded in a 6-well plate and transfected with pYES1L-CMV-PEDV-BGH and pCAGGS-PEDV-N plasmids at 70–90% confluency, and the supernatant was harvested 48 h after freeze-thawing. The cell supernatant was added to monolayer-grown Vero cells and infected with 3 μ g/ml trypsin for 48 h. The cells were then freeze-thawed again to collect the supernatant and passaged blindly on Vero cells until clear cytopathic effects were observed.

Knockout cell lines establishment and validation

Refer to the method of Yang et al. [30], transfect Lenti-Cas9 plasmid and auxiliary plasmid into 293T cells to package lentivirus, collect the supernatant 48 h later and infect IPI-2I cells. Use 5 μ g/mL puromycin

Table 1. Primers of constructing PEDV infectious cloning.

Name	Sequence (5'-3')
1F	CCAAAATCAACGGGACTTTCCAAAATG
1R	CAAGCACCATATGGGAACGGTTCC
2F	AGTCTCTGACTAAGGACCTACACACA
2R	CAAACAGTAGGTATGGTAGTATGCATACACAAT
3F	CTGTGGTGTGGCTGTACGTGA
3R	TTCTGTGCGGTTACCTCCTTAACG
4F	AGGACAATGATGGCAAGGTGGTACA
4R	GGTCCTACAACCTCATGTATGTTGCAC
5F	GATTGGACTGATGTTTCTGACTACAGGT
5R	TGTGATGGGGTACACACATTGTGGT
6F	AACGTATGTGTTTAGAACCTTGCAATCTC
6R	ACCTGAACATCGGCTGAAAGAATG
7F	AGGTCCAAGAGGTTGTTAATTCGCA
7R	ACTAGAAGGCACAGTCGAGGCG

Table 2. Primers for identification of PEDV infectious clones.

Name	Sequence (5'-3')
p-1F	TTACGCTAGGGATAACAGGTAATATAGAACCCGAA
p-1 R	AAATTTCTGCATCATTGGCAAAAGC
p-2F	GCTTTTGACTTTGCAAGCTATGGAGG
p-2 R	CATCAATGGCCTTTGCTATGCCGC
p-3F	CAGGATTGCAAGAGCACATTGGG
p-3 R	ATCAGCAACGCCACTAGCATCAA
p-4F	CGGCAGTCAGTGCTACTAAGCTTAA
p-4 R	ACCACCGTATGAATCCTGGTTAGTAGC
p-5F	GCTCGCAGCATACTATGCAGATTGT
p-5 R	AACATTATGTGAGGTAAGCACAAA
p-6F	GAAGATTACGGCTTTGAGCAGTTG
p-6 R	AGCCTTCTTTAGACACATTCTCCCA
p-7F	ACTATAAGCGCTGTTCTAATGGCCG
p-7 R	AGGTTACATACATCGTCGCGATGAA
p-8F	TCCAGGGTAGTGCCATTACACTG
p-8 R	GCACAGATGCGTAAGGAGAAAATACCG

(catalogue number: ST551; Beyotime) for screening, and use the limited dilution method to screen monoclonal cells stably expressing Cas9 protein in a 96-well plate. Subsequently, construct Lenti-sgRNA-EGFP plasmid according to the sgRNA in Table 3, and transfect 293T cells to package lentivirus. Infect the IPI-2I cell line stably expressing Cas9 protein with the packaged virus liquid, and screen monoclonal gene knockout cells through green fluorescence labelling and limited dilution method. Finally, perform western blot analysis and gene sequencing verification on the screened cells.

Western blotting Phos-tag gel analysis

Refer to the method of Jia et al. [29], the cells were lysed and proteins were separated by SDS-PAGE. Proteins were transferred to Millipore nitrocellulose membranes (Sigma, San Francisco, CA), which were subsequently blocked for 2 h at 25°C with TBS containing 5% non-fat milk and 0.05% Tween 20. Membranes were incubated with the indicated primary and secondary antibodies and developed using an ECL chemiluminescence kit (Bio-Rad, Hercules, CA, USA). $MnCl_2$ and Phos-assay were added to the SDS-PAGE gel to prepare the Phos-tag gel, and the treated protein samples were electrophoresed. After electrophoresis, the gel was washed with EDTA solution, transferred onto a PVDF membrane, incubated

Table 3. The sgRNAs and identification primers used for gene knockout.

Name	Sequence (5'-3')
GSK3 α -sgRNA-F	CACCGAAGCCGCTCTGTCGGAGCCATGGG
GSK3 α -sgRNA-R	AAACCCCATGGCTCCGACAGACGGCTTC
GSK3 β -sgRNA-F	CACCGTGAAATGGGTCATTTGGTGTTG
GSK3 β -sgRNA-R	AAACCCACACAAATGACCCATTCCAC
GSK3 α -F	CTGCGCTCGGCGCCATGAGC
GSK3 α -R	TCCAGTTTGGGGAGGGAGAGTGAC
GSK3 β -F	TCTTTTAGGAGACAAGGATGGC
GSK3 β -R	CTGCAATACTTTCTTGATGGCA

with primary and secondary antibodies, and ECL reagent was used for colour development.

Co-immunoprecipitation (Co-IP)

Magnetic beads carrying protein A/G (catalogue no. HY-K0202; MCE, New Jersey, USA) were incubated with an appropriate antibody at 25°C for 2 h and washed three times in PBST (PBS with 0.5% Tween 20). The diluted cell lysate was incubated with the beads in a rotating mixer for 4 h, followed by washing thrice in PBST.

Immunofluorescence assay and confocal microscopy

Inoculate IPI-2I or Vero cells into a 24-well plate or confocal culture dish, then inoculate with PEDV or transfect with PEDV N protein expression plasmid. After 36 h, fix with 4% paraformaldehyde and permeabilize cells using pre-cooled methanol. Wash cells gently three times with pre-cooled PBS, block with 5% BSA for 30 minutes, and incubate overnight with diluted primary antibody at 4°C. Wash with PBS three times, add diluted fluorescently labelled secondary antibody at 25°C, and incubate for 1 hour. Finally, stain the cell nuclei with DAPI. Image using a laser confocal scanning microscope (LSM800; Carl Zeiss AG, Oberkochen, Germany).

RNA isolation and quantitative PCR

Total RNA was isolated from the cells using TRIzol reagent (Invitrogen) according to the manufacturer's instructions. The reverse transcription products were amplified in accordance with the manufacturer's specifications using a Stratagene Mx Real-Time quantitative PCR system [29] (Bio-Rad, Hercules, CA) and SYBR Green PCR Master Mix (Vazyme, Nanjing, China).

Prediction of protein phosphorylation sites and associated protein kinases

Import the amino acid sequence into the online program NetPhos (<https://services.healthtech.dtu.dk/services/NetPhos-3.1>) for prediction, and select Ser and Thr as the prediction sites.

Statistical analysis

Refer to the method of Jia et al. [29], all results are presented as three independent experiments with

consistent outcomes. Data were expressed as the mean \pm SD. Statistical tests were performed using Student's t-test in GraphPad Prism 8. Asterisks indicate the statistical significance: * $p < 0.05$, ** $p < 0.01$, and *** $p < 0.001$.

Results

The PEDV N protein is highly phosphorylated

To analyse the phosphorylation level of the PEDV N protein, we used a Phos-tag gel, distinguishing between phosphorylated and non-phosphorylated states. After transfecting the PEDV N protein expression plasmid into 293T or IPI-2I cells, the N protein was enriched using immunoprecipitation, treated with or without λ PPase, and the proteins were transferred to PVDF membranes for development after electrophoresis. As shown in Figure 1(a), the phosphorylation level of the N protein decreased significantly after phosphatase treatment. We used the NetPhos software to predict the phosphorylation regions of the N protein and found a region rich in Thr and Ser (Figure 1(b)), which contained typical SR repeat sequences and was highly conserved in PEDV

(Figure 1(c)). Therefore, we constructed a mutant plasmid of the N protein SR region and named it PEDV-N SRE, in which Thr/Ser was mutated to glutamic acid that cannot be phosphorylated (Figure 1(d)). The mutant plasmid was cotransfected with the wild-type plasmid into 293T cells. After protein enrichment by immunoprecipitation, Phos-tag gel analysis demonstrated that the phosphorylation level of the N protein was significantly decreased following mutation in the SR region (Figure 1(e)). Compared to the group treated with λ PPase, the N protein with mutations in the SR region still exhibited phosphorylation modifications, suggesting that there are additional phosphorylation sites on the N protein.

GSK3 α/β phosphorylation of the N protein SR motif

We predicted potential protein kinases for phosphorylation of the SR region using the NetPhos program (Figure 2(a)), constructed related eukaryotic expression plasmids, and co-transfected them with the FLAG-tagged PEDV N protein-expression plasmid into 293T cells for immunoprecipitation. Through screening, we

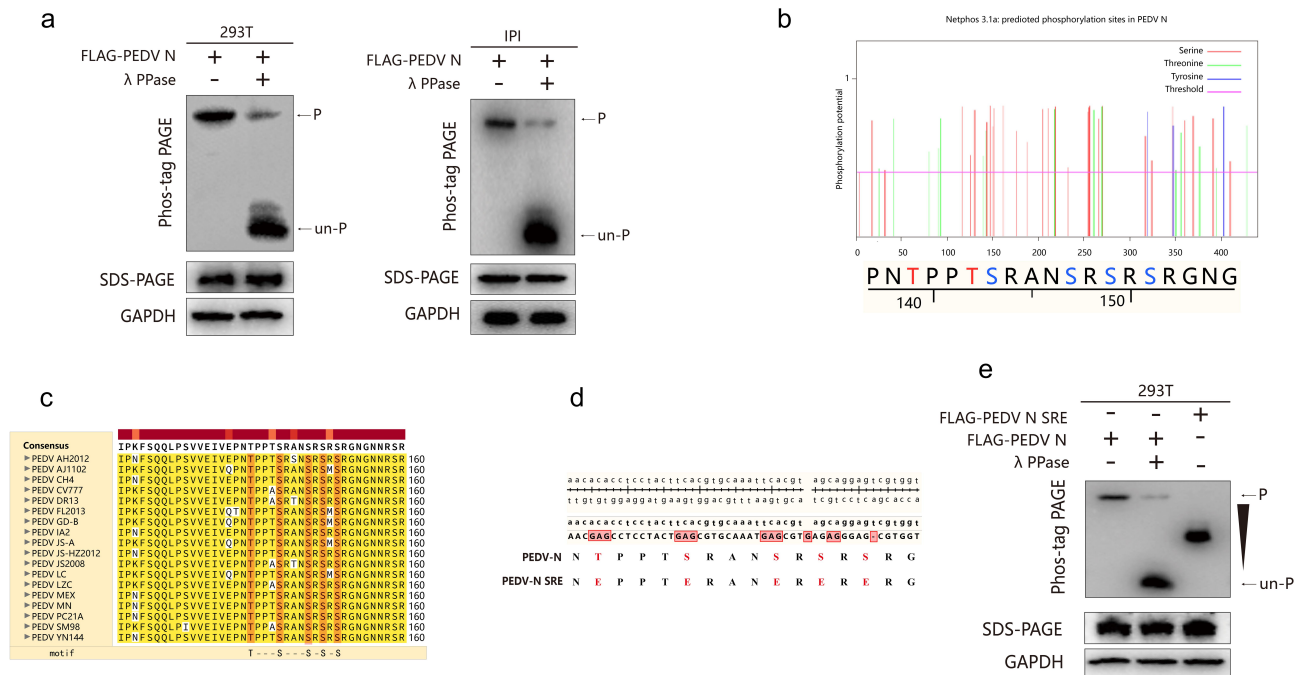


Figure 1. PEDV N protein is highly phosphorylated. (a) The plasmid expressing FLAG-PEDV N protein was transfected into 293T and IPI-2I cells. After 36 h, the cells were lysed using the cell lysis buffer. Immunoprecipitation (IP) of the lysate was performed using anti-FLAG beads, and the precipitated N protein was subjected to treatment with or without lambda protein phosphatase (λ PPase), followed by Western blotting and Phos-tag gel analysis. (b) The phosphorylation sites of PEDV N protein were predicted using the NetPhos program. (c) The N protein sequence alignment shows that the SR motif is highly conserved in PEDV. (d) Construction of plasmids targeting N protein SR motif mutations, in which the phosphorylation sites (Thr/Ser) were mutated to glutamic acid that cannot be phosphorylated. (e) The wild-type or SR motif of N protein mutant plasmids were transfected into 293T cells, the cells were lysed after 36 h for immunoprecipitation. As a control, precipitated wild-type N protein was treated with or without λ PPase, followed by Western blotting and Phos-tag gel analysis.

demonstrated that GSK3 α/β interacts with the N protein (Figure 2(b,c), Supplementary Fig. S1, Supplementary Fig. S2 AB). Furthermore, after mutation of the SR motif, the N protein no longer interacted with GSK3 β , and the interaction level with GSK3 α significantly reduced (Figure 2(d,e) Supplementary Fig. S2 CD). Laser confocal microscopy imaging indicated a clear co-localization of the N protein with GSK3 α/β in IPI-2I cells (Figure 2(f,g)). The colocalization of the N protein with GSK3 α/β significantly decreased after the mutation of the SR region (Figure 2f,g). These findings suggest that GSK3 α/β is involved in the phosphorylation of the N protein SR motif.

Inhibition of GSK3 α/β attenuates PEDV proliferation

To assess the impact of GSK3 α/β on PEDV proliferation, we selected four different GSK3 α/β inhibitors. First, cytotoxicity of the four inhibitors was evaluated using the CCK-8 assay in IPI-2I and Vero cells (Figure 3(a–h)). We chose doses with over 90% cell viability as safe doses: CHIR-99021 HCl (20 μ M), SB 216763 (20 μ M), TWS119 (20 μ M), and LiCl

(8 mm). After inoculating the cells with PEDV, the four inhibitors were added to Vero and IPI-2I cells at the specified concentrations, and 36 h later, the cell samples were collected for PEDV copy number detection and cell supernatant was assayed to determine the TCID₅₀. As shown in Figure 3(i–j), GSK3 α/β inhibitors significantly inhibited PEDV proliferation, with CHIR-99021 HCl having the most pronounced inhibitory effect. At the same time, detection of TCID₅₀ reached the same conclusion that CHIR-99021 HCl significantly inhibited the viral titre (Supplementary Fig. S3 AB). The effect of CHIR-99021 HCl on PEDV proliferation was independently verified using indirect immunofluorescence. As expected, CHIR-99021 HCl significantly inhibited the proliferation of PEDV in Vero and IPI-2I cells (Figure 3(k,l)).

Knockout of GSK3 α/β suppresses PEDV proliferation

To evaluate the effect of GSK3 α/β on PEDV proliferation, we used the CRISPR-Cas9 system to create cell

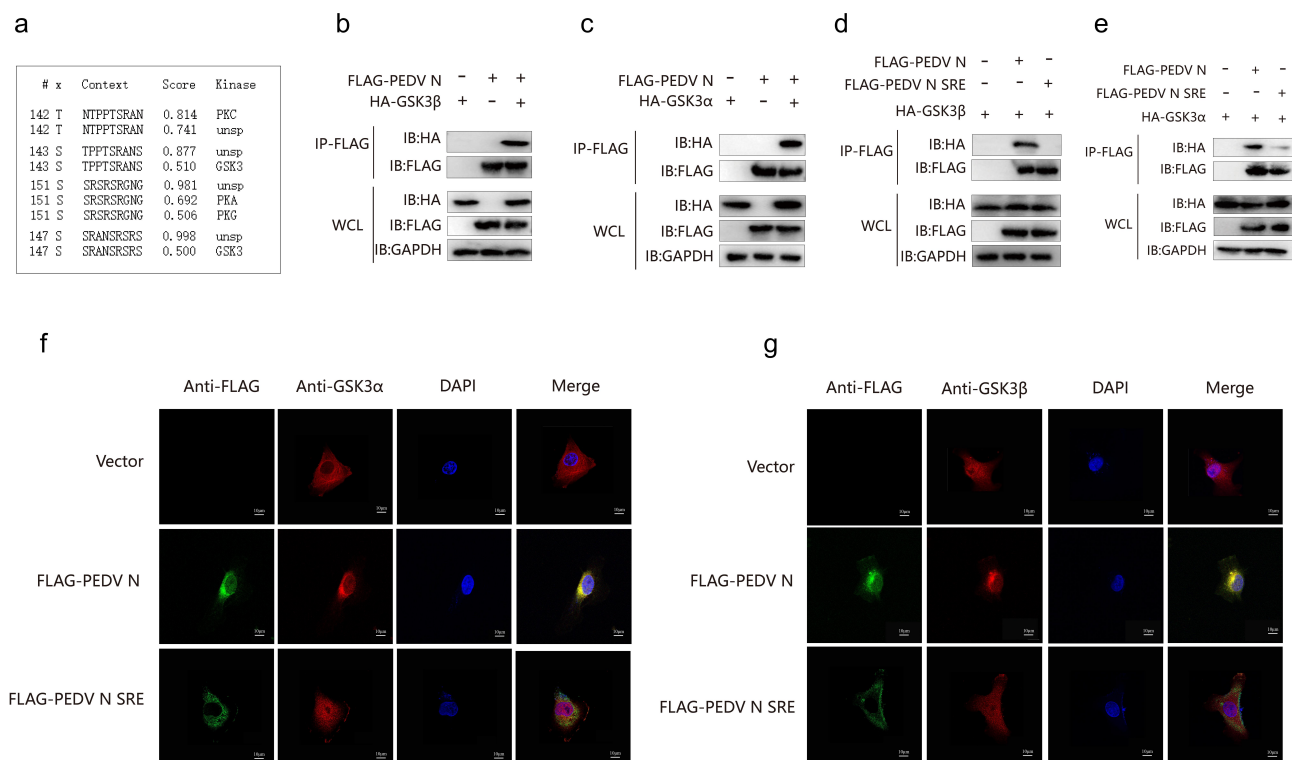


Figure 2. GSK3 α/β phosphorylation of the SR region of protein N. (a) NetPhos software was used for prediction of protein kinases that phosphorylate the SR motif of PEDV N protein. PKC, protein kinase C; PKA, protein kinase A; PKG, protein kinase G; GSK3, Glycogen synthase kinase 3. (b–e) 293T cells were co-transfected with FLAG-tagged wild-type or mutant N protein SR motif and HA-GSK3 α/β expression plasmids, immunoprecipitation was performed using FLAG antibody-labelled beads, and interactions were analysed by Western blotting. (f) and (g) the plasmid coding for FLAG-PEDV N or FLAG-PEDV N SRE protein was transfected into IPI-2I cells, with an empty vector plasmid used as the control. The cells were fixed with 4% formaldehyde after 36 h. The confocal laser microscopy was used to observe the colocalization of N protein (green) and GSK3 α/β (red).

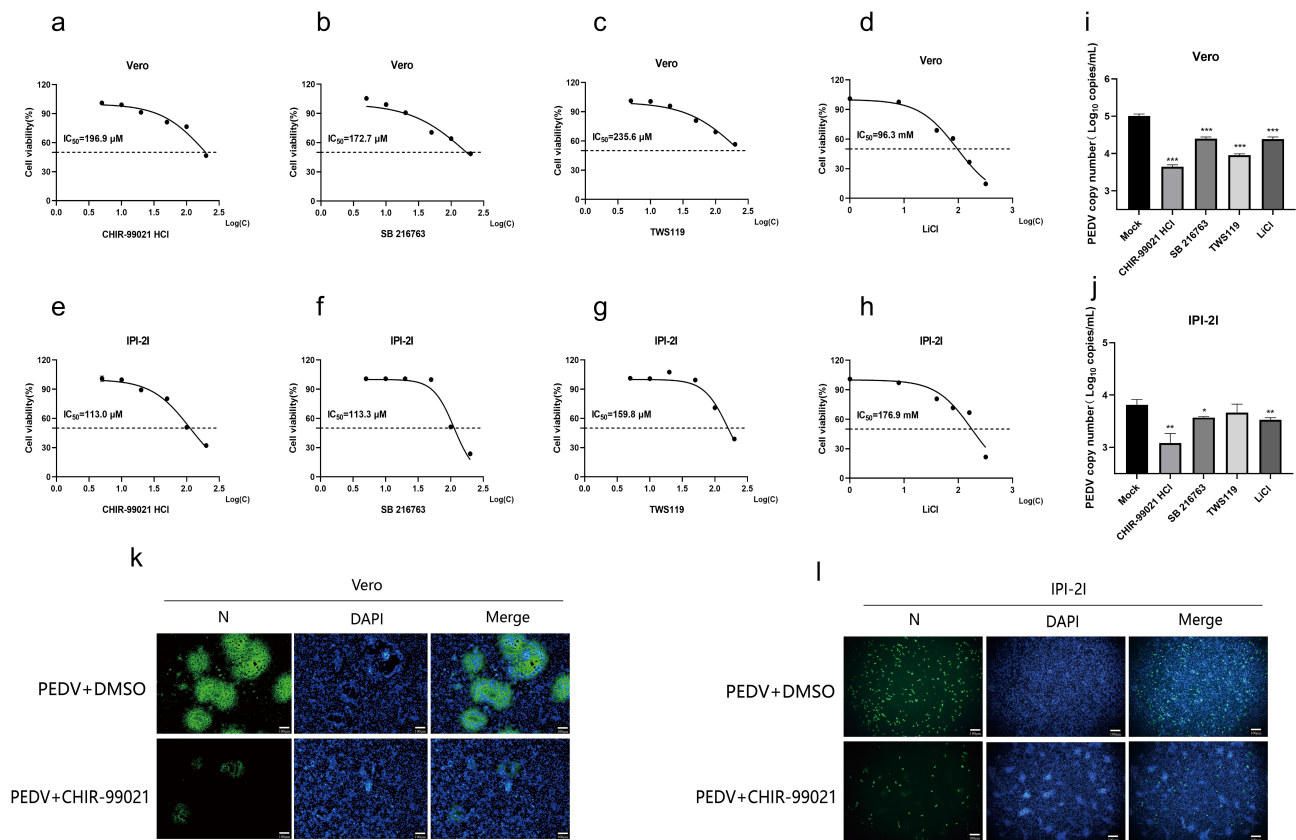


Figure 3. GSK3 α/β inhibitors impede the proliferation of PEDV. (a-d) Vero cells were cultured in a 96-well plate for 24 h. The reagents were added at various dilutions, and Vero cells were treated for 36 h. Then, following the manufacturer's instructions, 10 μ l of CCK-8 solution was added and incubated for 1 h to measure the absorbance at OD450. Relative cell viability = (average OD450 drug)/(average OD450 control). Use GraphPad to calculate the IC_{50} value. Data are expressed as the mean \pm SD of three independent experiments. (e-h) according to (a-d), the IPI-2I cells were processed the same way. Data are expressed as the mean \pm SD of three independent experiments. (i-j) Vero or IPI-2I cells were inoculated with PEDV at MOI of 0.01, and the experimental group was treated with 20 μ M of CHIR-99021 HCl, SB 216763, TWS119, or 8 mM LiCl, with DMSO as a blank control. Total RNA was extracted for viral copy number determination after 36 h. (k-l) Vero or IPI-2I cells were infected with PEDV at MOI of 0.01, and DMSO or CHIR-99021 HCl were added for co-culture during 36 h. Subsequently, 4% paraformaldehyde was used for fixation, and PEDV N protein (green) was detected through immunofluorescence. Data are representative of three independent experiments with three biological replicates (mean \pm SD). Asterisks indicate statistical significance calculated by Student t test: * p < 0.05, ** p < 0.01, *** p < 0.001.

lines deficient in GSK3 α/β using sgRNA from Table 3. The cell lines were analysed using Western blotting and gene sequencing (Figure 4(a,b)) to confirm that the target gene did not express the desired protein. Then, PEDV was inoculated onto wild-type and knockout cell lines at MOI of 0.01, and 36 h later, the expression of PEDV N protein was assessed. As shown in Figure 4(c,d) after knockout of GSK3 α/β , PEDV proliferation decreased significantly. We also measured the corresponding viral copy number, revealing that the loss of GSK3 β had a greater impact on PEDV proliferation than the loss of GSK3 α (Figure 4(e,f)), indicating that GSK3 β plays a key role in the phosphorylation of PEDV viral proteins. Detection of the viral titre also reached the same conclusion (Supplementary Fig. S3 CD). This was confirmed using indirect immunofluorescence

staining (Figure 4(g)). PEDV was inoculated onto wild-type and knockout cell lines, and viral infection levels were assessed using indirect immunofluorescence. As shown in Figure 4(g), PEDV infection decreased after the knockout of GSK3 α/β . After replenishing GSK3 α/β in the knockout cell lines, the proliferation of the virus was similar to the wild type (Figure 4(e,f) Supplementary Fig. S3 CD).

Construction of PEDV reverse genetics system and rescue of N protein SR region mutant strains

Reverse genetic systems are the key tools for viral research and vaccine development. Therefore, we used yeast recombination technology to construct a reverse genetics platform for PEDV (Figure 5(a)). The rescued

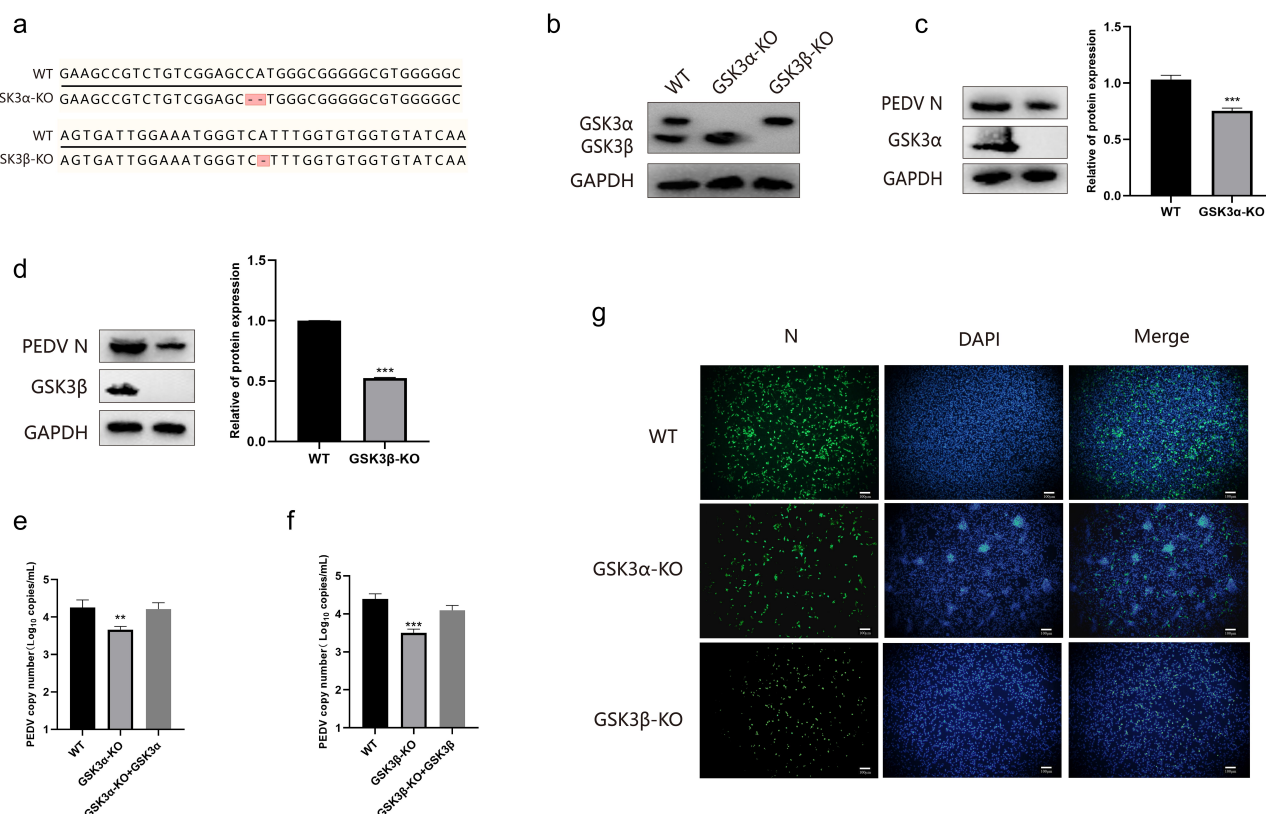


Figure 4. Knocking out GSK3α/β promotes the proliferation of PEDV. (a) Gene alignment of IPI-2I wild-type and GSK3α/β knockout cell lines. (b) The expression of GSK3α/β in IPI-2I wild-type and knockout cell lines assessed by Western blot analysis. (c-d) PEDV was inoculated on wild-type and GSK3α/β knockout IPI-2I cells at MOI of 0.01, and after 2 h, the medium was replaced with a DMEM base medium containing 3 μg/ml trypsin. After 36 h, cell samples were collected for a Western blotting to detect the expression level of PEDV N protein. The right image shows the greyscale analysis of the protein bands. (e-f) Wild-type, knockout, and rescue cells were handled the same way as they were in (c-d), and the total cellular RNA was extracted 36 h later to determine the viral copy number. (g) In wild-type and GSK3α/β-knockout IPI-2I cells, PEDV was inoculated at an MOI of 0.01. After 2 h, the medium was replaced with DMEM base medium containing 3 μg/ml trypsin. After 36 h, the cells were fixed with 4% paraformaldehyde, and PEDV N protein (green) was detected by immunofluorescence. Data are representative of three independent experiments with three biological replicates (mean ± SD). Asterisks indicate statistical significance calculated by Student t test: * $p < 0.05$, ** $p < 0.01$, *** $p < 0.001$.

and wild-type viruses were inoculated onto Vero cells, and analyses using immunofluorescence, Western blotting, and viral multistep growth curves confirmed that the rescued viruses were indistinguishable from the parental viruses (Figure 5(b-d)). This indicates that we successfully established a reverse genetics system for PEDV.

Based on a prior exploration of PEDV N protein phosphorylation, we introduced mutations into the SR region of the PEDV N protein using the PEDV reverse genetics system. As shown in Figure 1(d), Thr and Ser residues were mutated to prevent further phosphorylation. To better observe viral rescue, we independently expressed the EGFP protein in genome (Figure 5(e)). The EGFP gene is linked to the upstream of the N gene via the T2A sequence, allowing both to be expressed independently without influencing each other. The

EGFP protein does not participate in viral assembly and serves solely as an infection marker. Using the aforementioned rescue approach, we successfully rescued the recombinant virus containing SR region mutations and named them rPE-N SRE (Figure 5(f)). When Vero cells were infected with the wild-type and mutant strains at an MOI of 1, and their multistep growth curves were determined, it was observed that the SR motif mutant strains proliferated significantly slower than the wild-type strain (Figure 5(g)).

Discussion

Post-translational modifications of viral proteins are important factors that affect viral replication and infection, with phosphorylation as the primary modification.

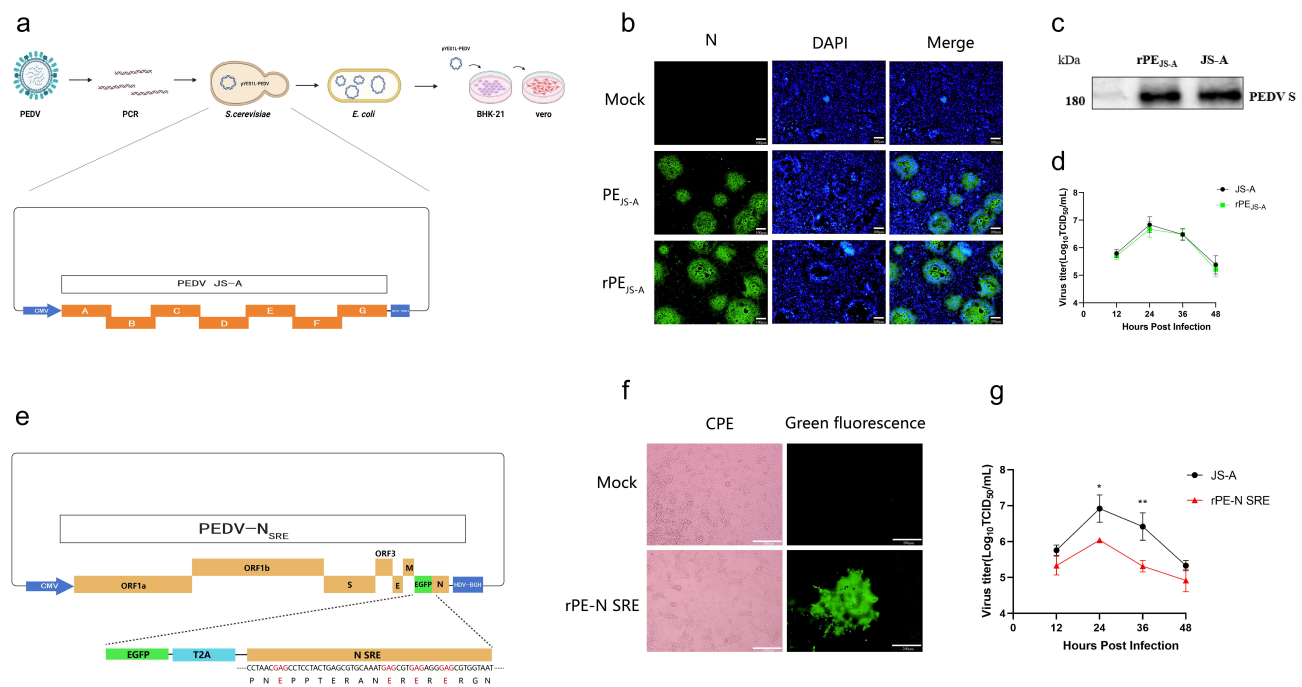


Figure 5. Mutations in the SR motif of the N protein attenuate the proliferation of PEDV. (a) Construction of infectious PEDV clone. The PEDV genome was divided into seven fragments, with adjacent fragments sharing approximately 200 nucleotides of overlapping regions. The seven fragments were co-transferred into MaV203 competent yeast cells using a linearized vector (pYES1L) that included CMV promoter and the HDV-BGH termination sequence, and positive colonies were screened by PCR. Plasmids from positive colonies were extracted and electroporated into DH10B competent cells for large-scale amplification. The amplified plasmids and the pCAGGS-PEDV N plasmid were co-transfected into BHK21 cells using Lipofectamine 3000, and the supernatant was collected to infect Vero cells 48 h after transfection. The rescued virus was serially passaged in Vero cells until significant cytopathic effects were observed. (b) To detect the N protein of the recombinant virus through indirect immunoassay, the recombinant and wild-type virus was inoculated onto Vero cells, fixed with 4% paraformaldehyde 24 h post-infection, and then incubated with anti-PEDV N protein mAb and Alexa Fluor 488-conjugated goat anti-mouse IgG (h + l). (c) Western blotting was used to identify the S protein of the recombinant virus. Vero cells were infected with the wild strain (JS-A) and the recombinant strain (rPE_{JS-A}) at MOI of 0.01, and after 24 h, the cells were lysed using a cell lysis buffer to detect the expression of PEDV S protein by Western blotting. (d) The multistep growth curves of the wild-type and recombinant strains. Vero cells were inoculated with PEDV JS-A and rPE_{JS-A} at MOI of 1. Cell supernatants were collected at 12, 24, 36, and 48 hpi for TCID₅₀ determination. (e) Construction of mutated strains containing PEDV N protein SR motif. Fragments containing the EGFP and N gene SR motif mutations were co-transferred into MaV203 competent yeast cells with six other fragments and a linearized vector. Following the method described in (a), the PEDV recombinant strain containing the SR motif mutation was finally rescued. (f) Observation of lesions of SR motif mutant strains using microscopy. (g) Multistep growth curves of wild-type strains and SR motif mutant strains. Vero cells were inoculated with wild-type strains and SR motif mutant strains at MOI of 1, and cell supernatants were collected at 12, 24, 36, and 48 hpi for TCID₅₀ determination. Data are representative of three independent experiments with three biological replicates (mean ± SD). Asterisks indicate statistical significance calculated by Student t test: * $p < 0.05$, ** $p < 0.01$, *** $p < 0.001$.

Viruses hijack the host phosphorylation system to reversibly phosphorylate viral proteins, thereby regulating their stability, activity, and interactions with other proteins [31]. For example, HIV-1 P6 can be phosphorylated by MAPK and ERK-2. After mutating the 23rd Thr residue of the P6 protein, the virus showed reduced infectivity and budding defects [32]. Phosphorylation of Ser/Thr125 in enterovirus 2A protease contributes to its proteolytic activity [33]. Additionally, a small number of viruses encode their own protein kinases [34]. These kinases can phosphorylate host or viral proteins, thereby affecting viral replication and assembly within host cells [35]. Some

viral kinases undergo autophosphorylation, which influences their catalytic activity by altering enzyme conformation. For example, rotavirus NSP5 and EBV BGLF4 proteins show autophosphorylation activity [36,37].

Since the onset of the COVID-19 pandemic, research on the pathogenic mechanisms of coronaviruses has been intensified. Phosphoproteomic analysis of SARS-CoV-2 provides important reference points for screening anti-coronavirus drugs [38]. In the analysis of viral protein phosphorylation, approximately 70 phosphorylation sites have been identified, mostly

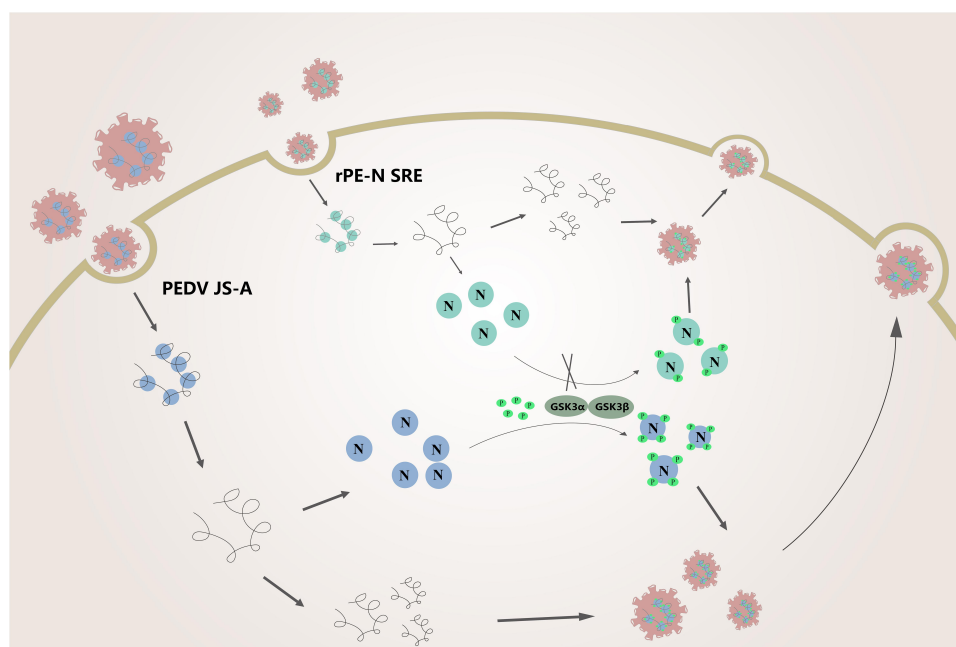


Figure 6. GSK3 α/β phosphorylation of PEDV N protein SR region promotes viral proliferation. The SR region mutant rPE-N_{SRE} cannot be phosphorylated by GSK3 α/β , resulting in weakened viral proliferation.

concentrated on the N and S proteins[39]. The SR region of the N protein contains a GSK3 α/β recognition site, common to most coronaviruses, suggesting a shared mechanism of GSK3 α/β involvement in the phosphorylation of the coronavirus N protein [9]. While not all cases of phosphorylation have clear effects on the viral life cycle, studying specific phosphorylation sites helps to understand the role of viral proteins in infected cells. The phosphorylation level of the N protein regulates its RNA-binding activity, subcellular localization, and polymerization capacity [10,12,15]. The focus of this study on the N protein SR region effectively demonstrates the role of N protein phosphorylation levels in viral infection and proliferation.

We also show that phosphorylation of the N protein by GSK3 α/β is indispensable. Blocking the expression of GSK3 α/β effectively inhibits the proliferation of PEDV. Through the screening of four inhibitors, we found that CHIR-99021 HCl had the greatest impact on PEDV proliferation, which could be related to its binding efficiency towards the target. Additionally, using reverse genetics techniques, the rescue of SR region-mutated viruses intuitively reflects the role of SR motif phosphorylation in the viral life cycle (Figure 6). It remains unclear whether the phosphorylation level of SR region affects the host recognition and response to viral proteins, which will be a direction for future research. In summary, our data suggests that targeting GSK3 α/β can inhibit PEDV virus proliferation, providing new insights into PEDV prevention and control.

Acknowledgements

We thank Prof. Lisheng Zhang from the College of Veterinary Medicine, Huazhong Agricultural University for providing the IPI-2I cells.

Funding

This work was supported by the National Natural Science Foundation of China [grant number 32072845].

Disclosure statement

No potential conflict of interest was reported by the author(s).

Data availability statement

The data that support the findings of this study are openly available in <https://doi.org/10.6084/m9.figshare.28129688>

Author contributions

All authors read and approved the final version of the manuscript. Research concepts and design were contributed by Zili Li. Experiments were conducted and data collected by Xiangchao Jia, Jing Chen, Chenxi Li, Jian Li, Min Su, Kang Yang, and Yang Zhang. Statistical analysis and data interpretation were performed by Xiangchao Jia and Jing Chen. The manuscript was drafted and revised by Xiangchao Jia and Jing Chen, with critical revisions by Zili Li. All authors agree to be accountable for all aspects of the work.

Glossary

PEDV:	porcine epidemic diarrhoea virus
GSK3 α/β :	glycogen synthase kinase 3 α/β
N:	nucleocapsid protein
IBV:	infectious bronchitis virus
MHV:	mouse hepatitis virus
DDX1:	DEAD box proteins
SARS:	severe acute respiratory syndrome
SARS-CoV-2:	severe acute respiratory syndrome coronavirus 2
BAC:	bacterial artificial chromosomes
cDNA:	complementary DNA
DMEM:	dulbecco's modified eagle medium
FBS:	foetal bovine serum
mAb:	monoclonal antibodies
λ PPase:	lambda protein phosphatase
EGFP:	Enhanced Green Fluorescent Protein
PBS:	phosphate buffered saline
DAPI:	diamidino-2-phenylindole dihydrochloride
MOI:	multiplicity of infection

ORCID

Zili Li  <http://orcid.org/0000-0002-9729-1339>

References

- [1] Shah M, Woo HG. Molecular perspectives of SARS-CoV-2: pathology, immune evasion, and therapeutic interventions. *Mol Cells*. 2021;44(6):408–421. doi: 10.14348/molcells.2021.0026
- [2] Shan D, Johnson JM, Fernandes SC, et al. N-protein presents early in blood, dried blood and saliva during asymptomatic and symptomatic SARS-CoV-2 infection. *Nat Commun*. 2021;12(1):1931. doi: 10.1038/s41467-021-22072-9
- [3] De Haan CAM, Rottier PJM. Molecular interactions in the assembly of coronaviruses. *Adv Virus Res*. 2005;64:165–230.
- [4] Chang C, Hou M, Chang C, et al. The SARS coronavirus nucleocapsid protein – forms and functions. *Antiviral Res*. 2014;103:39–50. doi: 10.1016/j.antiviral.2013.12.009
- [5] Huang Q, Yu L, Petros AM, et al. Structure of the N-Terminal RNA-Binding domain of the SARS CoV nucleocapsid protein. *Biochemistry*. 2004;43(20):6059–6063. doi: 10.1021/bi036155b
- [6] Fan H, Ooi A, Tan YW, et al. The nucleocapsid protein of coronavirus infectious bronchitis virus: crystal structure of its N-terminal domain and multimerization properties. *Structure (Lond Engl: 1993)*. 2005;13(12):1859–1868. doi: 10.1016/j.str.2005.08.021
- [7] Jayaram H, Fan H, Bowman BR, et al. X-ray structures of the N- and C-terminal domains of a coronavirus nucleocapsid protein: implications for nucleocapsid formation. *J Virol*. 2006;80(13):6612–6620. doi: 10.1128/JVI.00157-06
- [8] Luo H, Chen J, Chen K, et al. Carboxyl terminus of severe acute respiratory syndrome coronavirus nucleocapsid protein: self-association analysis and nucleic acid binding characterization. *Biochemistry*. 2006;45(39):11827–11835. doi: 10.1021/bi0609319
- [9] Liu X, Verma A, Gustavo Garcia J, et al. Targeting the coronavirus nucleocapsid protein through GSK-3 inhibition. *Proc Natl Acad Sci USA*. 2021;118(42):e2113401118. doi: 10.1073/pnas.2113401118
- [10] Stohlman SA, Fleming JO, Patton CD, et al. Synthesis and subcellular localization of the murine coronavirus nucleocapsid protein. *Virology*. 2004;130(2):527. doi: 10.1016/0042-6822(83)90106-X
- [11] Calvo E, Escors D, López JA, et al. Phosphorylation and subcellular localization of transmissible gastroenteritis virus nucleocapsid protein in infected cells. *J Gen Virol*. 2005;86(8):2255–2267. doi: 10.1099/vir.0.80975-0
- [12] Chen H, Gill A, Dove BK, et al. Mass spectroscopic characterization of the coronavirus infectious bronchitis virus nucleoprotein and elucidation of the role of phosphorylation in RNA binding by using surface plasmon resonance. *J Virol*. 2005;79(2):1164–1179. doi: 10.1128/JVI.79.2.1164-1179.2005
- [13] Lin L, Shao J, Sun M, et al. Identification of phosphorylation sites in the nucleocapsid protein (N protein) of SARS-coronavirus. *Int J Mass Spectrom*. 2007;268(2–3):296–303. doi: 10.1016/j.ijms.2007.05.009
- [14] White TC, Yi Z, Hogue BG. Identification of mouse hepatitis coronavirus A59 nucleocapsid protein phosphorylation sites. *Virus Res*. 2007;126(1–2):139–148. doi: 10.1016/j.virusres.2007.02.008
- [15] Surjit M, Kumar R, Mishra RN, et al. The severe acute respiratory syndrome coronavirus nucleocapsid protein is phosphorylated and localizes in the cytoplasm by 14-3-3-mediated translocation. *J Virol*. 2005;79(17):11476–11486. doi: 10.1128/JVI.79.17.11476-11486.2005
- [16] Wu C, Chen P, Yeh S. Nucleocapsid phosphorylation and RNA helicase DDX1 recruitment enables coronavirus transition from discontinuous to continuous transcription. *Cell Host Microbe*. 2014;16(4):462. doi: 10.1016/j.chom.2014.09.009
- [17] Surjit M, Lal SK. The SARS-CoV nucleocapsid protein: a protein with multifarious activities. *Infect Genet Evol*. 2008;8(4):397–405. doi: 10.1016/j.meegid.2007.07.004
- [18] Wu C, Yeh S, Tsay Y, et al. Glycogen synthase kinase-3 regulates the phosphorylation of severe acute respiratory syndrome coronavirus nucleocapsid protein and viral replication. *J Biol Chem*. 2009;284(8):5229–5239. doi: 10.1074/jbc.M805747200
- [19] Li C, Li Z, Zou Y, et al. Manipulation of the porcine epidemic diarrhea virus genome using targeted RNA recombination. *PLOS ONE*. 2013;8(8):e69997. doi: 10.1371/journal.pone.0069997
- [20] Beall A, Yount B, Lin C, et al. Characterization of a pathogenic full-length cDNA clone and transmission model for porcine epidemic diarrhea virus strain PC22A. *MBio*. 2016;7(1):e01451–01415. doi: 10.1128/mBio.01451-15
- [21] Fan B, Yu Z, Pang F, et al. Characterization of a pathogenic full-length cDNA clone of a virulent porcine epidemic diarrhea virus strain AH2012/12 in China. *Virology*. 2017;500:50–61. doi: 10.1016/j.virol.2016.10.011

- [22] Li J, Jin Z, Gao Y, et al. Development of the full-length cDNA clones of two porcine epidemic diarrhea disease virus isolates with different virulence. *PLOS ONE*. 2017;12(3):e0173998. doi: [10.1371/journal.pone.0173998](https://doi.org/10.1371/journal.pone.0173998)
- [23] Zhou Y, Li C, Ren C, et al. One-step assembly of a porcine epidemic diarrhea virus infectious cDNA clone by homologous recombination in yeast: rapid manipulation of viral genome with CRISPR/Cas9 gene-editing technology. *Front Microbiol*. 2022;13:787739. doi: [10.3389/fmicb.2022.787739](https://doi.org/10.3389/fmicb.2022.787739)
- [24] Silva JV, Arenhart S, Santos HF, et al. Efficient assembly of full-length infectious clone of Brazilian IBVDV isolate by homologous recombination in yeast. *Braz J Microbiol*. 2014;45(4):1555–1563. doi: [10.1590/S1517-83822014000400054](https://doi.org/10.1590/S1517-83822014000400054)
- [25] Gibson DG, Benders GA, Axelrod KC *et al*. One-step assembly in yeast of 25 overlapping DNA fragments to form a complete synthetic *Mycoplasma genitalium* genome. *Proc Natl Acad Sci U S A*. 2008;105(51):20404–20409 doi:[10.1073/pnas.0811011106](https://doi.org/10.1073/pnas.0811011106)
- [26] Joska TM, Mashruwala A, Boyd JM, et al. A universal cloning method based on yeast homologous recombination that is simple, efficient, and versatile. *J Microbiol Methods*. 2014;100:46–51. doi: [10.1016/j.mimet.2013.11.013](https://doi.org/10.1016/j.mimet.2013.11.013)
- [27] Guo J, Li F, He Q, et al. Neonatal fc receptor-mediated IgG transport across porcine intestinal epithelial cells: potentially provide the mucosal protection. *DNA Cell Biol*. 2016;35(6):301–309. doi: [10.1089/dna.2015.3165](https://doi.org/10.1089/dna.2015.3165)
- [28] Qian S, Zhang W, Jia X, et al. Isolation and identification of porcine epidemic diarrhea virus and its effect on host natural immune response. *Front Microbiol*. 2019;10:2272. doi: [10.3389/fmicb.2019.02272](https://doi.org/10.3389/fmicb.2019.02272)
- [29] Jia X, Chen J, Qiao C, et al. Porcine epidemic diarrhea virus nsp13 protein downregulates neonatal fc receptor expression by causing promoter hypermethylation through the NF- κ B signaling pathway. *J Immunol*. 2023;210(4):475–485. doi: [10.4049/jimmunol.2200291](https://doi.org/10.4049/jimmunol.2200291)
- [30] Yang K, Dong J, Li J, Zhou R, Jia X, Sun Z, Zhang W, Li Z and Wobus C E. (2025). The neonatal Fc receptor (FcRn) is required for porcine reproductive and respiratory syndrome virus uncoating. *J Virol*, 99(1), [10.1128/jvi.01218-24](https://doi.org/10.1128/jvi.01218-24)
- [31] Jakubiec A, Jupin I. Regulation of positive-strand RNA virus replication: the emerging role of phosphorylation. *Virus Res*. 2007;129(2):73–79. doi: [10.1016/j.virusres.2007.07.012](https://doi.org/10.1016/j.virusres.2007.07.012)
- [32] Hemonnot B, Cartier C, Gay B, et al. The host cell MAP kinase ERK-2 regulates viral assembly and release by phosphorylating the p6gag protein of HIV-1 *. *J Biol Chem*. 2004;279(31):32426–32434. doi: [10.1074/jbc.M313137200](https://doi.org/10.1074/jbc.M313137200)
- [33] Wang Y, Zou W, Niu Y, et al. Phosphorylation of enteroviral 2Apro at ser/Thr125 benefits its proteolytic activity and viral pathogenesis. *J Med Virol*. 2022;95(1):e28400. doi: [10.1002/jmv.28400](https://doi.org/10.1002/jmv.28400)
- [34] He Z, He YS, Kim Y, et al. The human cytomegalovirus UL97 protein is a protein kinase that autophosphorylates on serines and threonines. *J Virol*. 1997;71(1):405. doi: [10.1128/jvi.71.1.405-411.1997](https://doi.org/10.1128/jvi.71.1.405-411.1997)
- [35] Cunningham C, Davison AJ, Dolan A, et al. The UL13 virion protein of herpes simplex virus type 1 is phosphorylated by a novel virus-induced protein kinase. *J Gen Virol*. 1992;73(2):303–311. doi: [10.1099/0022-1317-73-2-303](https://doi.org/10.1099/0022-1317-73-2-303)
- [36] Blackhall J, Fuentes A, Hansen K, et al. Serine protein kinase activity associated with rotavirus phosphoprotein NSP5. *J Virol*. 1997;71(1):138. doi: [10.1128/jvi.71.1.138-144.1997](https://doi.org/10.1128/jvi.71.1.138-144.1997)
- [37] Kato K, Kawaguchi Y, Tanaka M, et al. Epstein–Barr virus-encoded protein kinase BGLF4 mediates hyperphosphorylation of cellular elongation factor 1 δ (EF-1 δ): EF-1 δ is universally modified by conserved protein kinases of herpesviruses in mammalian cells. *J Gen Virol*. 2001;82(6):1457–1463. doi: [10.1099/0022-1317-82-6-1457](https://doi.org/10.1099/0022-1317-82-6-1457)
- [38] Bouhaddou M, Memon D, Meyer B, et al. The global phosphorylation landscape of SARS-CoV-2 infection. *Cell*. 2020;182(3):685. doi: [10.1016/j.cell.2020.06.034](https://doi.org/10.1016/j.cell.2020.06.034)
- [39] Chatterjee B, Thakur SS. SARS-CoV-2 infection triggers phosphorylation: potential target for anti-COVID-19 therapeutics. *Front Immunol*. 2022;13:829474. doi: [10.3389/fimmu.2022.829474](https://doi.org/10.3389/fimmu.2022.829474)